Direct exchange interaction of localized spins associated with unpaired *sp* electrons in Be-doped low-temperature-grown GaAs layers

K. W. Bae, Mohd Ambri Mohamed, D. W. Jung, and N. Otsuka[a)]
School of Materials Science Japan Advanced Institute of Science and Technology Asahidai 1-1, Nomishi, Ishikawa 923-1292, Japan

(Received 29 September 2010; accepted 22 February 2011; published online 11 April 2011)

Beryllium-doped GaAs layers grown at low temperatures by molecular-beam epitaxy contain localized spins associated with unpaired *sp* electrons of As_{Ga}^{+} ions. Interactions of these localized spins are investigated by measuring the magnetization with a superconducting quantum interference device and the peak-to-peak width of electron paramagnetic resonance (EPR) spectra for samples with different spin concentrations ranging from 3×10^{18} to 2.0×10^{19} cm^{-3}. The results show that localized spins in this material antiferromagnetically interact on each other via direct exchange. From the analysis of the temperature dependence and field dependence of the magnetization on the basis of the Curie–Weiss law and the molecular-field approximation, exchange energy of each sample was derived. The dependence of the exchange energy on the concentration of localized spins is reasonably explained by a model of direct exchange, which results from the overlapping of wave functions of unpaired electrons at As_{Ga}^{+} ions. The peak-to-peak width of EPR spectra increases with an increase in the spin concentration at low temperatures, whereas it decreases with an increase in the temperature for samples with high spin concentrations. These EPR results also show that significant exchange interactions indeed occur between localized spins in this material. These effects of direct exchange interactions between localized spins can clearly be observed at their average distances of around 4 nm, which implies a considerably large spatial extension of the wave function of an unpaired *sp* electron around an As_{Ga}^{+} ion. © *2011 American Institute of Physics*. [doi:10.1063/1.3567914]

I. INTRODUCTION

In the past decade, a variety of spin-related phenomena in solids have been explored by both experimental and theoretical studies, which have been driven mainly by a possibility of the development of a technology field called spintronics. One such phenomenon is collective magnetism based on localized spins associated with unpaired *sp* electrons in materials without magnetic elements. In the investigation of this phenomenon, many studies have focused on localized spins associated with unpaired *sp* electrons, which form at native point defects such as vacancies in semiconductors and insulators.[1–12] These unpaired *sp* electrons are fairly localized and hence are expected to carry local magnetic moments at substantially high temperatures.

Because of a number of reports of the observation of ferromagnetism at room temperature, which have been attributed to the aforementioned unpaired *sp* electrons,[2,5,6,11,12] there have been active theoretical investigations on localized spins associated with these unpaired electrons with an expectation of the development of an unconventional class of magnetic systems. A number of electronic structure calculations predicted the preference of ferromagnetic interactions of these localized spins in the systems, where room-temperature ferromagnetism was reported to occur.[1,3,4,7–10,12] Recent studies, however, pointed out the necessity of great care in such a prediction, as the sufficient inclusion of electron correlation in calculations often leads to a very different situation for localized spins at point defects with enhanced localization of carriers of magnetic moments and structural distortion.[13–15] In experimental studies, the occurrence of the observed room-temperature ferromagnetism was found to be highly dependent on the sample-preparation process. In some cases ferromagnetism was not observed in a system from which other groups reported the observation.[16,17]

The difficulty in the investigation of these localized spins reflects the inherent properties of native point defects. Unlike unpaired *d* and *f* electrons of magnetic elements, unpaired *sp* electrons in solids result from specific configurations of atoms around native point defects. In addition, native point defects, in general, have high formation energies and hence may sensitively change their structures depending on the environment. It is, therefore, not evident whether localized spins exist at given point defects in a real system, even if a qualitative chemical bond picture predicts their existence. The aforementioned properties also make interactions of these localized spins to occur in a highly complicated manner in comparison to those of unpaired *d* and *f* electrons of magnetic elements; the coexistence of point defects at a close distance may result in a significant change in their structure and hence influence interactions of localized spins. High formation energies of native point defects also make it difficult to introduce a high concentration of defects in a closely controlled manner, which is necessary for the experimental investigation of their interactions.

[a)]Author to whom correspondence should be addressed. Electronic mail: ootsuka@jaist.ac.jp. FAX: 81-761-51-1149.

In the situation described earlier, it is worthwhile to experimentally investigate a selected system in order to find fundamental characteristics of localized spin systems associated with native point defects. Some of the characteristics may be significantly different from those of unpaired *d* and *f* electron systems. Finding of such fundamental characteristics may enable one to explore a possibility of the development of these localized spins as an unconventional magnetic system, which exhibit a variety of spin-related phenomena. In this paper we present results of a study on localized spins in Be-doped GaAs layers grown at low temperatures (LT-GaAs) by molecular-beam epitaxy (MBE), in which we have investigated how localized spins associated with native point defects interact on each other. The most important characteristic that distinguishes localized spins in Be-doped LT-GaAs from those associated with native point defects in other materials is that the concentration of localized spins can be closely controlled by the growth process as explained in the following.

A LT-GaAs layer contains a high concentration of antisite arsenic (As_{Ga}) atoms whose concentration depends on the growth temperature.[18] The electronic structure of an As_{Ga} atom has been investigated by many theoretical studies in the past in connection with the EL2 defect in GaAs.[19–23] It was shown that the As_{Ga} defect induced three bound states of A_1 symmetry, among which one fell deep in the band gap and was a twofold occupation in the neutral state.[19,20,23] In nondoped LT-GaAs, a few As_{Ga} atoms change into As_{Ga}^{+} ions due to the compensation by Ga vacancies.[24] These As_{Ga}^{+} ions carry magnetic moments associated with unpaired *sp*-type electrons that were detected by a number of past studies with the electron paramagnetic resonance (EPR)[25] and magnetic circular dichroism of absorption.[26] LT-GaAs, therefore, is considered as a system where the existence of localized spins at native point defects has been fully confirmed. In earlier studies on LT-GaAs, the concentration of As_{Ga}^{+} ions was found to be increased by doping a high concentration of Be atoms, which compensate As_{Ga} atoms in place of Ga vacancies.[27,28] In a recent study, we grew thick Be-doped LT-GaAs layers with thicknesses up to 20 μm and observed their magnetic moments with a superconducting quantum interference device (SQUID).[29] The field dependence of the magnetization of these layers at low temperatures was approximately described by the Brillouin function, and a few samples exhibited maxima in the temperature dependence of the magnetization at low temperatures, the origin of which, however, is not known at present.

In the present study we have made close analyses of results of SQUID and EPR measurements for samples with different spin concentrations ranging from 3×10^{18} to 2.0×10^{19} cm^{-3} in order to clarify the mechanism of interactions of localized spins in this material. The results show that localized spins in this material antiferromagnetically interact on each other via direct exchange. From the analysis of the temperature dependence and field dependence of the magnetization on the basis of the Curie–Weiss law and the molecular-field approximation, an exchange energy of each sample were derived. The dependence of the exchange energy on the concentration of localized spins is reasonably explained by a model of direct exchange, which results from the overlapping of the wave functions of unpaired electrons at As_{Ga}^{+} ions. The peak-to-peak width of EPR spectra increases with an increase in the spin concentration at low temperatures, whereas it decreases with an increase in the temperature for samples with high spin concentrations. These EPR results also show that significant exchange interactions indeed occur between localized spins in this material. The noteworthy finding in the present study is that the effects of direct exchange interactions between localized spins can clearly be observed at their average distances around 4 nm, which implies a considerably large spatial extension of the wave function of an unpaired *sp* electron around an As_{Ga}^{+} ion.

II. EXPERIMENT

Beryllium-doped LT-GaAs layers were grown by utilizing a conventional MBE system. Semi-insulating epiready (100)GaAs wafers were used as substrates. After desorption of an oxide layer of the substrate surface, a 150-nm-thick GaAs buffer layer was grown at 580 °C, followed by the growth of an AlAs layer and a 75-nm-thick GaAs buffer layer at the same temperature. The growth of the AlAs layer was made for the lift-off process of LT-GaAs layers.[30] The substrate temperature was subsequently lowered for the growth of a Be-doped LT-GaAs layer. The growth temperature and the Be-doping concentration were varied among samples. Nearly the same atom flux ratio of As to Ga, being around 5,[18] was used for the growth of all samples.

Table I list substrate temperatures T_s, Be concentrations [Be], thicknesses t, and spin concentrations N_s of Be-doped LT-GaAs layers investigated in the present study. For samples 1–4, Weiss temperatures θ are also listed. The Be concentrations were estimated by using the Be effusion cell temperature for which uniformly doped layers were grown at 520 °C and their hole concentrations were measured for given Be effusion cell temperatures. The substrate temperature for the growth of a LT-GaAs layer was estimated by extrapolating the reading of a thermocouple at desorption of the oxide layer on the substrate surface. It is widely known to be difficult to estimate accurate substrate temperatures for the low-temperature MBE growth. According to our earlier study,[18] for a given thermocouple reading an actual substrate temperatures varies over ± 10 °C due to a small change in

TABLE I. Substrate temperature T_s, Be concentration [Be], thickness t, and spin concentrations N_s of samples 1–9. For samples 1–4, Weiss temperatures θ are also listed.

Number	T_s (°C)	[Be] (10^{19}/cm^3)	t (μm)	[N_s] (10^{19}/cm^3)	θ (K)
1	260	2.4	18	1.91	0.34
2	260	2.6	18	2.26	0.45
3	280	2.7	15	1.42	0.16
4	255	2.9	18	1.99	0.31
5	270	2.9	3	2.06	—
6	275	2.5	8	1.88	—
7	220	5.5	1.4	0.91	—
8	260	5.5	4	0.67	—
9	240	5.5	2.3	0.32	—

the contact between a substrate and a substrate holder and that between a substrate holder and a thermocouple. Samples whose substrate temperatures are the same with each other in Table I, therefore, were not necessarily grown at the same temperature.

The magnetization of samples 1–4 was measured by SQUID, whereas samples 4–9 were used for EPR measurements. For the SQUID measurement, Be-doped LT-GaAs layers with thicknesses ranging from 15 to 18 μm were grown in order to gain sufficient magnetic moments of samples, whereas thinner samples were used solely for the EPR measurement. For all samples listed in Table I, a reflection high-energy electron diffraction pattern indicating the two-dimensional growth mode was maintained until the end of the growth. For the growth of thick samples from 1 to 4, relatively high substrate temperatures ranging around 270 °C were used in order to avoid the breakdown of the layer-by-layer growth due to surface roughening. At typical substrate temperatures around 200 °C for the growth of a LT-GaAs layer, the breakdown occurs around 1 μm.[31] Details of the growth process of thick Be-doped LT-GaAs layers were described in an earlier paper.[29] Spin concentrations N_s and Weiss temperatures θ of samples 1–4 were estimated by the analysis of their magnetization as explained in the next section. Spin concentrations of samples 5–9 were estimated with EPR spectra by using sample 4 as a reference whose spin concentration was determined by the analysis of the magnetization. As seen in Table I, samples 7–9, whose Be concentrations are considerably higher than those of other samples have low spin concentrations. The low spin concentrations in these three samples may be attributed to the occupation of interstitial sites by Be atoms, which results in the compensation of acceptor Be atoms at substitutional sites for high Be-doping concentrations. The verification of this explanation, however, requires further experimental study.

The crystalline quality of samples were analyzed by x-ray diffraction and cross-sectional transmission electron microscopy (TEM). For the measurement with the EPR system and SQUID, a LT-GaAs layer was lifted off from a GaAs substrate by etching the AlAs layer with a solution of HF acid.[30] EPR measurements were carried out with an *X*-band spectrometer at 9.6 GHz. For the SQUID measurements 24 sheets of the LT-GaAs layer with 3×3 mm^2 size were wrapped in a thin plastic sheet and installed in a straw used as a sample holder of SQUID. In order to avoid an inclusion of a small piece of magnetic material, the lift-off process and installation of a sample in the SQUID sample holder were carefully carried out with plastic tweezers.

III. RESULTS AND DISCUSSION

A. Magnetization

All four samples used for the SQUID measurement have nearly defect-free single crystalline LT-GaAs layers, which were confirmed by XRD and TEM analyses. Figures 1(a) and 1(b) are cross-sectional TEM bright-field images of sample 4. The former image was taken from an area close to the AlAs layer, which appears as a bright band, whereas the latter image was taken from an area close to the layer surface.

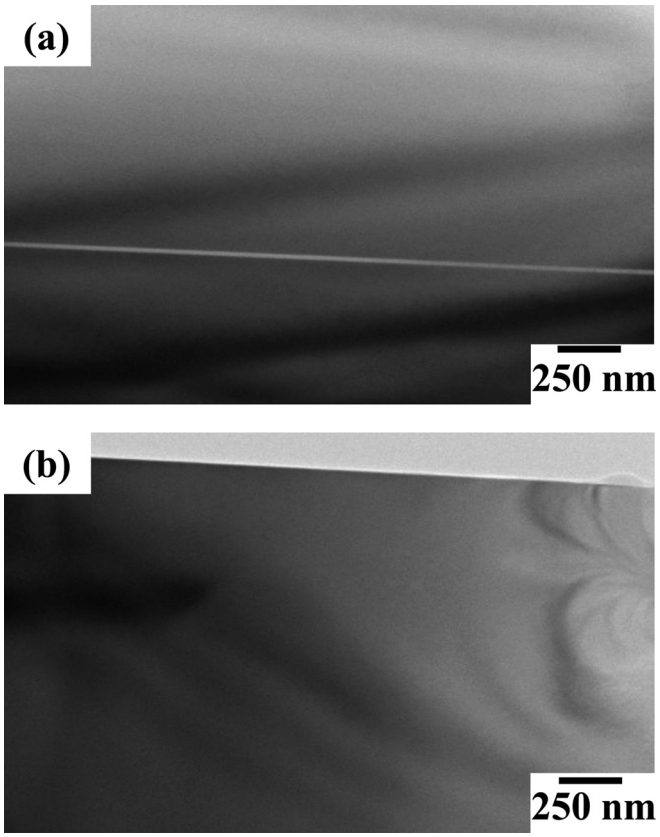

FIG. 1. Cross-sectional TEM bright-field images of sample 4.

These images show a single crystalline structure without any extended defect from the bottom to the top of the 18-μm-thick LT-GaAs layer.

The magnitude of a magnetic moment of a Be-doped LT-GaAs sample at a low temperature is comparable to those of a plastic film and a straw, which were used as a sample holder for the SQUID measurement. As shown in our earlier paper with measured magnetic moments,[29] the temperature dependence of the magnetic moments of the plastic film and straw is negligible in comparison to that of a Be-doped LT-GaAs sample as expected from their diamagnetic properties. For the analysis of the magnetization, therefore, the contribution of the plastic film and straw to a measured magnetic moment for a given temperature T was removed by subtracting a magnetic moment measured at a high temperature, 30 K. Figure 2(a) is the temperature dependence of the magnetization of sample 4, which was measured at 0.1 T after zero-field cooling. Because of the subtraction of a magnetic moment measured at 30 K and the division by the volume of the Be-doped LT-GaAs sample, the plots correspond to the difference between the magnetization of a sample at T and 30 K. Figure 2(b) is the field dependence of the magnetization of sample 4 for three temperatures, 1.8, 4.5, and 10 K. Similarly to Fig. 2(a), the plots correspond to the difference between the magnetization at T and 100 K.

With the measured results shown in Fig. 2(a) the magnetization of a sample at each temperature T was estimated by using the following equation:

$$M(T) = M^{\exp}(T) - M^{\exp}(30\ \mathrm{K}) + M^{\mathrm{para}}(30\ \mathrm{K}), \quad (1)$$

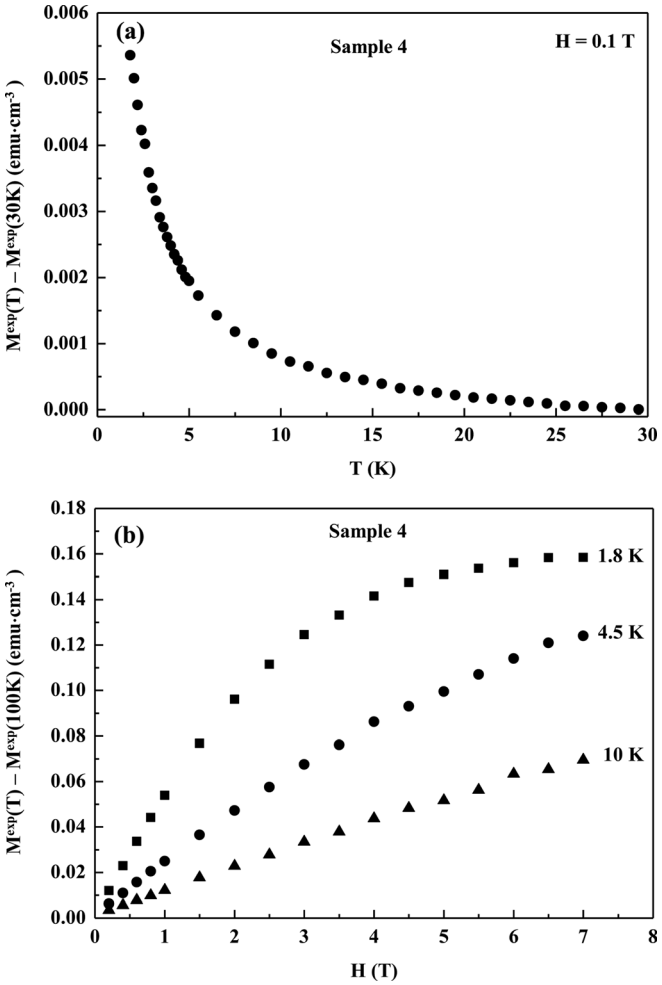

FIG. 2. (a) Temperature dependence of the magnetization $M^{exp}(T) - M^{exp}(30\ K)$ and (b) field dependence of the magnetization $M^{exp}(T) - M^{exp}(100\ K)$ of sample 4.

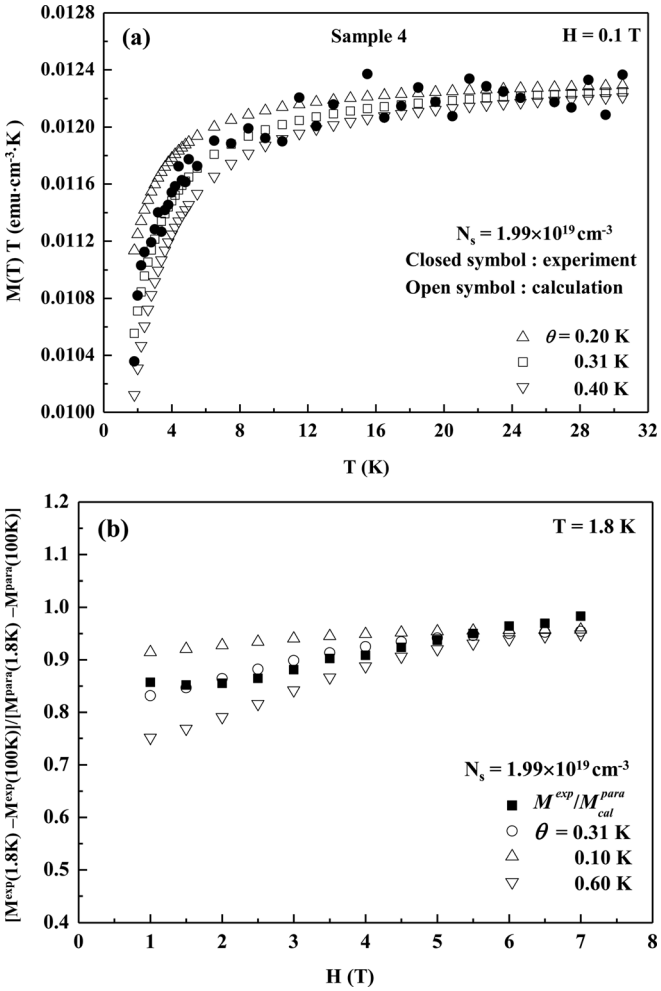

FIG. 3. (a) Plots $M(T)T$ at 0.1 T for sample 4 as a function of T. The fitting of calculated values based on the Curie–Weiss law was made for different values of θ. (b) Plots of $[M^{exp}(1.8\ K) - M^{exp}(100\ K)]/[M^{para}(1.8\ K) - M^{para}(100\ K)]$ of sample 4 as a function of the magnetic field. Calculated values $[M^{AF}(1.8\ K) - M^{AF}(100\ K)]/[M^{para}(1.8\ K) - M^{para}(100\ K)]$ are plotted for different values of θ.

where $M^{exp}(T)$ and $M^{exp}(30\ K)$ are the measured magnetization at T and 30 K, respectively. The last term in Eq. (1) is the calculated magnetization based on the Curie paramagnetism:

$$M^{para}(T) = N_s S g \mu_B B_s\left(\frac{S g \mu_B H}{k_B T}\right), \tag{2}$$

where $B_s(x)$ is the Brillouin function. In the equation, N_s, S, g, μ_B and H are the spin concentration, the localized spin, Landé g factor, Bohr magneton, and the magnetic field, respectively. As explained in the following, the effect of interactions of localized spins in these samples is negligibly small at 30 K. With $M(T)$ obtained from Eq. (1), next $M(T)T$ was plotted as a function of T. Figure 3(a) shows the plots $M(T)T$ at 0.1 T for sample 4. For the estimation of M^{para} (30 K), 1/2 and 2.04 were used for values of S and g, which were derived in an earlier EPR study on As^{+}_{Ga} ions in LT-GaAs.[25] The value of the spin concentration N_s was chosen so as to make $M(T)T$ to fluctuate around a constant value in the high-temperature range, where large fluctuations of $M(T)T$ at high temperatures are due to very small values of $M^{exp}(T) - M^{exp}$ (30 K) in that temperature range. If a larger value of N_s is used, $M(T)$ shows an explicit tendency of a continuous increase with the temperature even in the high temperature range, whereas a smaller value results in the opposite tendency. By judging with these tendencies, N_s was determined as $1.99 \pm 0.3 \times 10^{19}\text{cm}^{-3}$ for sample 4.

The plots of $M(T)T$ in Fig. 3(a) show an increasing reduction at lower temperatures, suggesting antiferromagnetic interactions between localized spins. The fitting of calculated values based on the Curie–Weiss law

$$M^{CW}(T) = \frac{CW}{T + \theta}, \tag{3}$$

where

$$C = N_s S(S+1) g^2 \mu_B^2 / 3k_B$$

was made for different values of θ as shown in Fig. 3(a). For the calculation the same value of N_s was used. The value of θ was uniquely determined for a given N_s by fitting the calculated curve to $M(T)T$ in the temperature range from 2 to 6 K, where the plots exhibit a large curvature. For sample 4, θ is estimated as 0.31 ± 0.03 K.

Two parameters, N_s and θ, were also estimated simultaneously by using the nonlinear curve fitting with the equation of the Curie–Weiss law. The value N_s estimated in this way is $(1.980 \pm 0.004) \times 10^{19}\text{cm}^{-3}$, which is very close to the value estimated in the first method. The value of θ determined by the nonlinear curve fitting, however, deviates significantly from the aforementioned value of 0.31 K and makes large fluctuations if data points of 1.8 or 2.0 K are excluded from the fitting, indicating the difficulty in the determination of θ by the nonlinear curve fitting. As seen in Fig. 3(a), these two data points are significantly apart from other data points, whereas data points measured in the temperature range from 2.2 to 8.5 K form a nearly continuous and monotonic curve. If the fitting is made by excluding the above two data points, θ becomes a value close to 0.31 K with N_s nearly unchanged and does not vary significantly with a change of the temperature range used for the fitting. Values of θ determined in the first method, therefore, are used for the analysis of interactions of localized spins in this study, whereas values of N_s were estimated by the nonlinear curve fitting.

In order to substantiate the result of the previous analysis, the field dependence of the magnetization of a sample was compared with the calculated one in the molecular-field approximation. In Fig. 3(b), $[M^{\text{exp}}(1.8\text{ K}) - M^{\text{exp}}(100\text{ K})]/[M^{\text{para}}(1.8\text{ K}) - M^{\text{para}}(100\text{ K})]$ of sample 4 is plotted as a function of the magnetic field. The subtraction of $M^{\text{exp}}(100\text{ K})$ was made in order to remove the contribution of the sample holder. The division by the calculated paramagnetic magnetization M^{para} enables one to observe clearly the effect of antiferromagnetic exchange interactions. In the molecular field approximation,[32] the magnetization M^{AF} of an antiferromagnetic crystal in the magnetic field H at a temperature above the Néel temperature is given by

$$M^{\text{AF}}(T,H) = N_s S g \mu_B B_s \left[\frac{S g \mu_B (-AM^{\text{AF}} + H)}{k_B T}\right], \tag{4a}$$

where

$$A = \frac{2}{g^2 \mu_B^2 N_s} \sum_m J(R_m). \tag{4b}$$

Here, $J(R_m)$ is the exchange energy and the summation is taken over nearest-neighbor spins located at R_m with respect to the reference spin. In the case of Be-doped LT-GaAs localized spins are randomly distributed, and hence the magnitude of J varies continuously over a certain range. In the present analysis, one exchange energy, which corresponds to that for the average interval of localized spins, is used. With this approximation, the parameter A is related to θ by $A = \theta/C$. In Fig. 3(b), calculated values $[M^{\text{AF}}(1.8\text{ K}) - M^{\text{AF}}(100\text{ K})]/[M^{\text{para}}(1.8\text{ K}) - M^{\text{para}}(100\text{ K})]$ are plotted for different values of θ. In the calculation, the spin concentration N_s derived from the above-mentioned analysis was used. Figure 3(b) shows that the field dependence of the magnetization can be reasonably reproduced with a value close to 0.31 K for θ, implying the fairly good consistency of the present analysis. The small difference between the experimental curve and the calculated one with 0.31 K for θ may be attributed to the simplified molecular-field approximation used in the calculation. It was also found that the use of Eq. (4a) in place of Eq. (2) for the calculation of $M(T)$ in Eq. (1) with the estimated values of N_s and θ did not cause any significant change in the previous results.

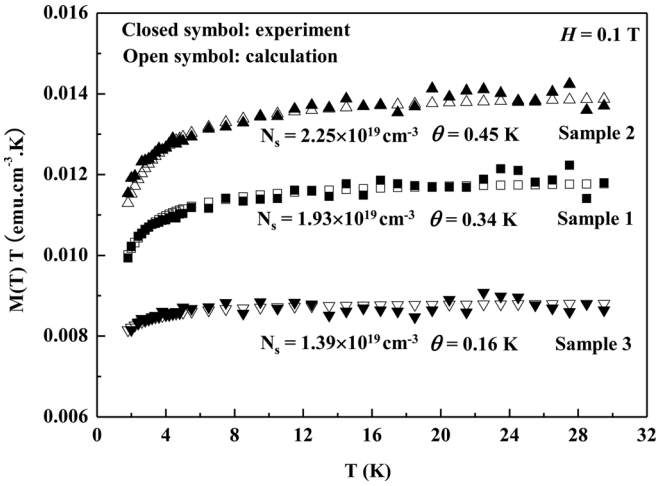

FIG. 4. Plots of $M(T)T$ for samples 1–3 along with calculated curves with the most appropriate values of N_s and θ.

Figure 4 shows plots of $M(T)T$ for samples 1–3 along with calculated curves with the most appropriate values of N_s and θ. Values of N_s were determined by the nonlinear curve fitting, and those of θ were estimated by the method used for sample 4 because of the reason explained earlier. Samples 2 and 3 have larger and smaller values for N_s and θ than those of sample 4, respectively, whereas sample 1 has a similar value with the latter one. These estimated values are listed in Table I for each sample.

B. EPR linewidth

The linewidth of EPR spectra changes sensitively by exchange interactions of localized spins.[33] Even weak exchange interactions whose effect on the magnetization can be observed only at low temperatures give rise to a significant effect on the linewidth at high temperatures. We, therefore, analyzed the linewidth of EPR spectra of Be-doped LT-GaAs layers.

All reported EPR spectra of As_{Ga} defects in GaAs including those in LT-GaAs have similar large linewidths irrespective of their concentrations.[25,34–38] An earlier optically detected electron-nuclear double resonance(ODENDOR) study on As_{Ga} defects indicated the significant distribution of an unpaired electron over four nearest-neighbor As atoms and large quadrupole interactions among these four As atoms and the $\text{As}_{\text{Ga}}^{+}$ ion.[39] Other experimental and theoretical studies showed large atomic displacements around an As_{Ga} atom.[40–42] The large linewidth is considered to be inherent to these properties of an isolated As_{Ga} defect. Because of the large linewidth for the isolated As_{Ga} defect, the detection of a change in the linewidth resulting from interactions of localized spins requires a close analysis of a spectrum curve. Among four hyperfine lines of As_{Ga} defects, the line that was observed at the highest magnetic field was

used for the analysis of the peak-to-peak linewidth. According to the Breit–Rabi formula,[43] the position of this line is separated from the nearest one by the largest distance and hence has the smallest effect of overlapping the tail of the nearest resonance peak. In the analysis, we also used a spectrum curve whose noises were removed by the Fourier-transform filtering in order to determine positions of the maximum and minimum of the curve accurately.

Figure 5(a) shows EPR spectra of samples 5 and 8, which correspond to the fourth hyperfine lines. The inset is the spectrum of sample 5, which includes all four hyperfine lines. The spectra of samples 5 and 8 were measured at 4.7 and 4.0 K, respectively. The positions of the maxima and minima of each curve are indicated by arrows in the figure. Peak-to-peak linewidths determined from these spectra are 37.6 and 31.2 mT for samples 5 and 8, respectively, where samples 5 and 8 have high and low spin concentrations, respectively, as listed in Table I. In Fig. 5(b), peak-to-peak linewidths determined for samples 4–9 are plotted as a function of the spin concentration. All EPR spectra used for this analysis were measured in the temperature range from 3.9 to 4.9 K. Figure 5(b) shows a clear tendency of an increase in the linewidth with the spin concentration, although these increases correspond to small fractions of the linewidth. The increase in the linewidth at low temperatures for higher spin concentrations is attributed to dipole interactions and crystal fields caused by neighboring localized spins.[33,44]

Figure 6(a) shows EPR spectra of sample 5 that were measured at 4.6 and 31.8K. Sample 5 has a higher spin concentration and hence has a large linewidth. As seen in Fig. 6(a), the peak-to-peak linewidth becomes smaller at a higher temperature. In Fig. 6(b), the linewidth is plotted as a function of the temperature for samples 5 and 6. In both cases, the linewidth decreases with an increase in the temperature and approaches the linewidths of samples with low spin concentrations. In a paramagnetic phase with antiferromagnetic interactions, the EPR linewidth is known to increase when the temperature is lowered toward the Neél temperature.[45] This result along with that in Fig. 5(b), therefore, implies that exchange interactions of localized spins occur in samples with high spin concentrations and reduce the effect of dipole interactions and the crystal field on the linewidth. Magnitudes of changes in the linewidth, which are several millitesla, are also found reasonable for the values of θ derived in the present analysis when they are compared

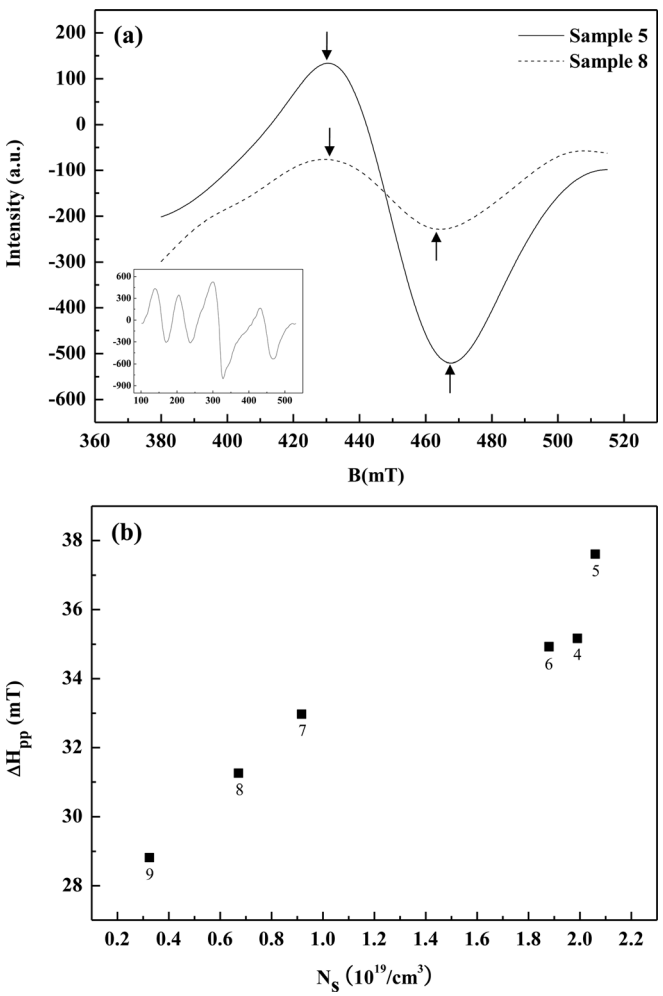

FIG. 5. (a) EPR spectra of samples 5 and 8, which correspond to the fourth hyperfine lines. The inset is the spectrum of sample 5, which includes all four hyperfine lines. (b) Plots of peak-to-peak linewidths determined for samples 4–9 as a function of the spin concentration.

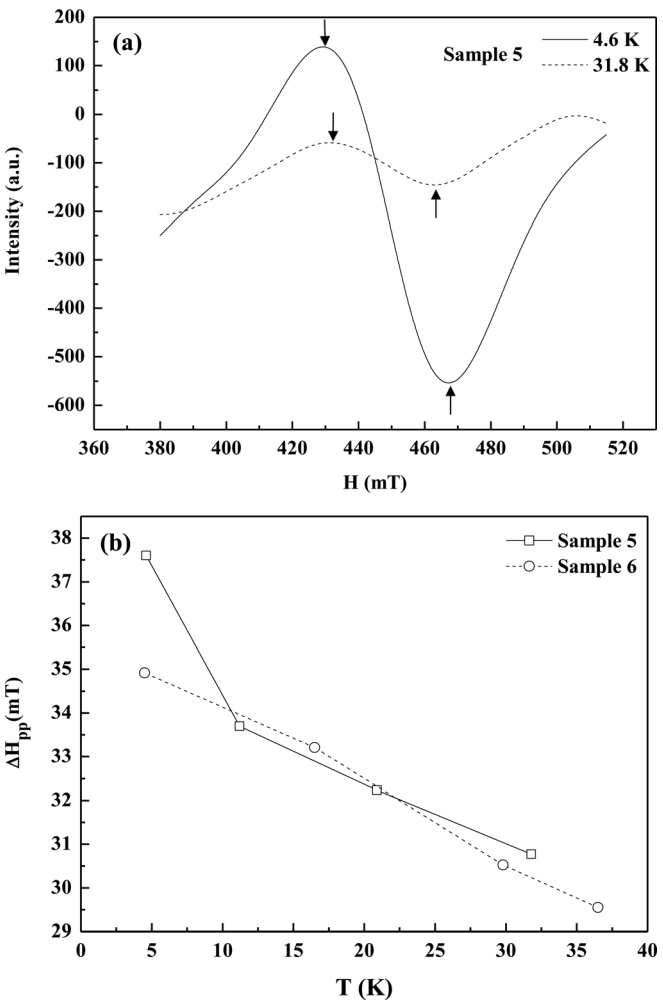

FIG. 6. (a) EPR spectra of sample 5, which were measured at 4.6 and 31.8 K. (b) Plots of linewidth as a function of the temperature for samples 5 and 6.

with earlier results of the exchange narrowing in other paramagnetic materials with antiferromagnetic interactions.[33]

C. Exchange interaction

The analysis of the magnetization and EPR linewidth has shown that localized spins interact on each other via antiferromagnetic exchange. Although many experimental studies on localized spins associated with native point defects have been reported recently, there has been no study that investigated localized spins in paramagnetic states by using samples with different spin concentrations in order to clarify the mechanism of their interactions. Many reported studies have focused only on the occurrence or absence of room-temperature ferromagnetism in samples.[2,5,6,11,12]

In the mean-field approximation, the exchange energy J can be estimated from θ via Eq. (4b) and the relation $A = \theta/C$. Because of random arrangements of localized spins in the present system, the estimated exchange energy J is considered as that for the average distance of localized spins. The number of neighboring spins is assumed to be six as in the case of a simple cubic structure. In Fig. 7, estimated exchange energies of four samples from 1 to 4 are plotted as a function of the average distance r_{av} in the logarithmic scale.

As expected from the values of θ, the exchange energy J changes significantly with a change of the average distance r_{av} which is $N_s^{-1/3}$. Although the arrangement of four data points deviates from a straight line to a certain extent, Fig.7 suggests that the exchange energy J changes exponentially with the average distance.

In the case of direct exchange, which results from overlapping of wave functions of two localized spins, the leading term of the exchange energy is of the order $\exp(-2\alpha R)$ times algebraic factors, where R is the nearest-neighbor distance and a wave function decays exponentially as $\exp(-\alpha r)$ at a large distance r.[46] By assuming the relation $J \propto \exp(-2\alpha r)$, the value of α, 0.88 nm^{-1}, is derived from Fig. 7 with the least square fitting. The reciprocal of α represents the spatial extension of the wave function because it corresponds to the Bohr radius in the case of the hydrogenic $1s$ wave function.

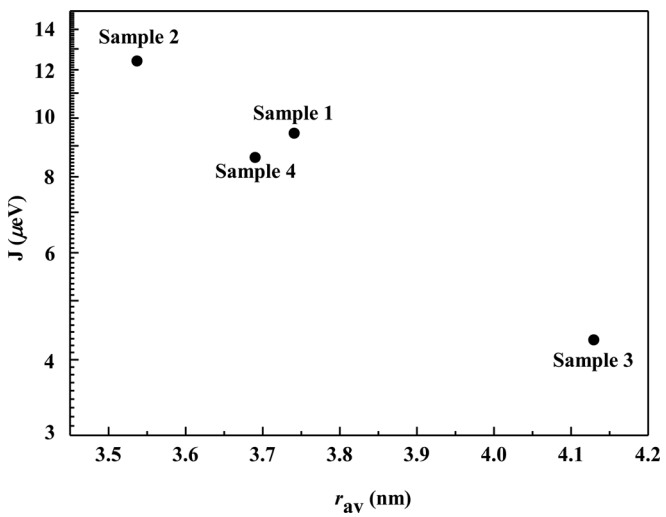

FIG. 7. Plots of estimated exchange energies J of four samples 1–4 as a function of the average distance r_{av}.

The value of α^{-1} which is 1.1 nm is considered to be reasonable for the extension of the wave function of a localized spin, as earlier experimental studies on As_{Ga} defects, such as those on ODENDOR[39] and hopping conduction[47] and theoretical studies on wave functions[20,23] suggested a similar extension of the wave function for an excess electron of the As_{Ga} defect. With these results, therefore, one can conclude that localized spins interact on each other via a direct exchange in Be-doped LT-GaAs in the range of these spin concentrations.

The average distances of localized spins in samples 1–4 range from 3.5 to 4.2 nm. The direct exchange interaction of localized spins, over this range of distances, results from a large spatial extension of wave functions of unpaired *sp* electrons. Similar direct exchange interactions occur in shallow-donor-doped semiconductors such as P-doped Si and In-doped CdS, which were investigated extensively in the past.[48–50] In comparison to localized spins in these shallow-donor-doped semiconductors, those in Be-doped LT-GaAs exist in a more complex structure resulting from the properties of native point defects. There are large lattice distortions around an As_{Ga} defect[40–42] and the existence of high concentrations of compensating Be^- ions and neutral As_{Ga} atoms along with As_{Ga}^+ ions. In addition, the wave function of an unpaired electron is not hydrogenic and its form directly depends on the configuration of atoms in the As_{Ga} defect.[20,23] It is, therefore, significant that with the present results one can consider Be-doped LT-GaAs as one spin system in which localized spins directly interact on each other similar to those in shallow-donor-doped semiconductors and those based on unpaired *d* and *f* unpaired electrons. As another interesting aspect suggested by the present results, Be-doped LT-GaAs can be considered as a Mott insulator with a single orbital per site, where excess electrons and holes can be introduced as neutral As_{Ga} atoms and As_{Ga}^{++} ions, respectively.

The concentration of As_{Ga} atoms in LT-GaAs is known to be increased to 1×10^{20} cm^{-3} by the growth at a temperature lower than those used in the present study.[18] If such a high concentration of As_{Ga} atoms can be converted to As_{Ga}^+ ions by Be doping, the exchange energy is expected to increase significantly and may result in the occurrence of a cooperative phenomenon of a spin system. There is, however, another possibility that As_{Ga} defects may change the structure and become nonmagnetic due to their interactions at a close distance. In order to investigate these possibilities one needs to find a method to prepare samples for the magnetization measurement by overcoming the problem of surface roughening in the growth of thick LT-GaAs layers at a low temperature.[31,51]

IV. CONCLUSION

In the present study we have made analyses of results of SQUID and EPR measurements for samples with different spin concentrations in order to clarify the mechanism of interactions of localized spins associated with native point defects. The results show that localized spins in this material antiferromagnetically interact on each other via direct exchange. From the analysis of the temperature dependence and field

dependence of the magnetization on the basis of the Curie–Weiss law and the molecular-field approximation, exchange energy of each sample was derived. The dependence of the exchange energy on the concentration of localized spins is reasonably explained by a model of direct exchange. The peak-to-peak width of EPR spectra increases with an increase in the spin concentration at low temperatures, whereas it decreases with an increase in the temperature for samples with high spin concentrations. These EPR results also show that significant exchange interactions indeed occur between localized spins in this material. The noteworthy finding is that the effects of direct exchange interactions between localized spins can clearly be observed at their large average distances around 4 nm, in spite of the presence of the large lattice distortion and high concentrations of Be^{-} ions.

[1]I. S. Elfimov, S. Yunoki, and G. A. Sawatzky, Phys. Rev. Lett. **89**, 216403 (2002).
[2]M. Venkatasan, C. B. Fitzgerald, and J. M. D. Coey, Nature, **430**, 630 (2004).
[3]C. D. Pemmaraju and S. Sanvito, Phys. Rev. Lett. **94**, 217205 (2005).
[4]J. Osorio-Guillén, S. Lany, S. V. Barabash, and A. Zunger, Phys. Rev. Lett. **96**, 107203 (2006).
[5]T. Dubroca, J. Hack, R. E. Hummel, and A. Angerhofer, Appl. Phys. Lett. **88**, 182504 (2006).
[6]N. H. Hong, J. Sakai, N. Poirot, and V. Brizé, Phys. Rev. B **73**, 132404 (2006).
[7]P. Dev, Y. Xue, and P. Zhang, Phys. Rev. Lett. **100**, 117204 (2008).
[8]Q. Wang, Q. Sun, G. Chen, Y. Kawazoe, and P. Jena, Phys. Rev. B **77**, 205411 (2008).
[9]Y. Gohda and A. Oshiyama, Phys. Rev. B **78**, 161201 (2008).
[10]H. Peng, H. J. Xiang, S.-H. Wei, S.-S. Li, J.-B. Xia, and J. Li, Phys. Rev. Lett. **102**, 017201 (2009).
[11]S. Chawla, K. Jayanthi, and R. K. Kotnala, Phys. Rev. B **79**, 125204 (2009).
[12]J. B. Yi, C. C. Lim, G. Z. Xing, H. M. Fan, L. H. Van, S. L. Huang, K. S. Yang, X. L. Huang, X. B. Qin, B. Y. Wang, T. Wu, L. Wang, H. T. Zhang, X. Y. Gao, T. Liu, A. T. S. Wee, Y. P. Feng, and J. Ding, Phys. Rev. Lett. **104** 137201 (2010).
[13]A. Droghetti, C. D. Pemmaraju, and S. Sanvito, Phys. Rev. B **78**, 140404 (2008).
[14]J. Winterlik, G. H. Fecher, C. A. Jenkins, C. Felser, C. Mühle, K. Doll, M. Jansen, L. M. Sandratskii, and J. Kübler, Phys. Rev. Lett. **102**, 016401 (2009).
[15]J. A. Chan, S. Lany, and A. Zunger, Phys. Rev. Lett. **103**, 016404 (2009).
[16]D. W. Abraham, M. M. Frank, and S. Guha, Appl. Phys. Lett. **87**, 252502 (2005).
[17]Y.-C. Chi, Y.-Y. Wei, J.-H. Chao, and Y. Liou, Appl. Phys. Lett. **93**, 036101 (2008).
[18]A. Suda and N. Otsuka, Appl. Phys. Lett., **73**, 1529 (1998).
[19]P. J. Lin-Chung and T. L. Reinecke, Phys. Rev. B **27**, 1101 (1983).
[20]G. B. Bachelet, M. Schlüter, and G. A. Baraff, Phys. Rev. B **27**, 2545 (1983).
[21]G. A. Baraff and M. Schlüter, Phys. Rev. Lett. **55**, 1327 (1985).
[22]D. J. Chadi and K. J. Chang, Phys. Rev. Lett. **60**, 2187 (1988).
[23]J. Dabrowski and M. Scheffler, Phys. Rev. B **40**, 10391 (1989).
[24]D. C. Look, in *Properties of Gallium Arsenide*, 3rd ed., edited by M. R. Brozel and G. E. Stillman (INSPEC, London, 1996), p. 684.
[25]H. J. von Bardeleben, M. O. Manasreh, D. C. Look, K. R. Evans, and C. E. Stutz, Phys. Rev. B **45**, 3372 (1992).
[26]Z. Liliental-Weber, W. Swider, K. M. Yu, J. Kortright, F. W. Smith, and A. R. Calawa, Appl. Phys. Lett. **58**, 2153 (1991).
[27]P. Specht, S. Jeong, H. Sohn, M. Lyusberg, A. Prasad, J. Gebauer, R. Krause- Rehberg, and E. R. Weber, Mater. Sci. Forum **258–263**, 951 (1997).
[28]A. Krotkus, K. Bertulis, L. Dapkus, U. Olin, and S. Marcinkevičius, Appl. Phys. Lett. **75**, 3336 (1999).
[29]D. W. Jung, J. P. Noh, and N. Otsuka, Physica B **405**, 4133 (2010).
[30]E. Yablonovitch, T. Gmitter, J. P. Harbison, and R. Bhat, Appl. Phys. Lett. **51**, 2222 (1987).
[31]D. J. Eaglesham, L. N. Pfeiffer, K. W. West, and D. R. Dykaar, Appl. Phys. Lett. **58**, 65 (1991).
[32]P. W. Anderson, in Solid State Physics, edited by H. Ehrenreich, F. Seitz, and D. Turnbull (Academic, New York, 1963), Vol. 14, p. 99.
[33]P. W. Anderson and P. R. Weiss, Rev. Mod. Phys. **25**, 269 (1953).
[34]N. K. Goswami, R. C. Newman, and J. E. Whitehouse, Solid State Commun. **40**, 473 (1981).
[35]E. R. Weber, H. Ennen, U. Kaufmann, J. Windscheif, J. Schneider, and T. Wosinski, J. Appl. Phys. **53**, 6140 (1982).
[36]J. Schneider and U. Kaufmann, Solid State Commun. **44**, 285 (1982).
[37]H. J. von Bardeleben, D. Stiévenard, D. Deresmes, A. Huber, and J. C. Bourgoin, Phys. Rev. B **34**, 7192 (1986).
[38]A. Mauger, H. J. von Bardeleben, J. C. Bourgoin, and M. Lannoo, Phys. Rev. B **36**, 5982 (1987).
[39]D. M. Hofmann, B. K. Meyer, F. Lohse, and J.-M. Spaeth, Phys. Rev. Lett. **53**, 1187 (1984).
[40]X. Liu, A. Prasad, J. Nishio, E. R. Weber, Z. Liliental-Weber, and W. Walukiewicz, Appl. Phys. Lett. **67**, 279 (1995).
[41]T. E. Staab, R. M. Nieminen, J. Gebauer, R. Krause-Rehberg, M. Luysberg, M. Haugk, Th. Frauenheim, Phys. Rev. Lett. **87**, 045504 (2001).
[42]S. Fukushima and N. Otsuka, J. Appl. Phys. **101**, 073513 (2007).
[43]G. Breit and I. I. Rabi, Phys. Rev. **38**, 2082 (1931).
[44]J. H. Van Vleck, Phys. Rev. **74**, 1168 (1948).
[45]M. S. Seehra, J. Appl. Phys. **42**, 1290 (1971).
[46]C. Herring, in Magnetism, Vol IIB, edited by G. T. Rado and H.Suhl (Academic, New York, 1966), p. 1.
[47]F. Shimogishi, K. Mukai, S. Fukushima, and N. Otsuka, Phys. Rev. B **65**, 165311 (2002).
[48]R. B. Kummer, R. E. Walstedt, S. Geschwind, V. Narayanamurti, and G. E. Devlin, Phys. Rev. Lett. **40**, 1098 (1978).
[49]K. Andres, R. N. Bhatt, P. Goalwin, T. M. Rice, and R. E. Walstedt, Phys. Rev. B **24**, 244 (1981).
[50]M. J. Hirsch, D. F. Holcomb, R. N. Bhatt, and M. A. Paalanen, Phys. Rev. Lett. **68**, 1418 (1992).
[51]G. Apostolopoulos, J. Herfort, L. Däweritz, K. H. Ploog, and M. Luysberg, Phys. Rev. Lett. **84**, 3358 (2000).